YOUR ARTICLE

Please review the proof* of your article carefully, checking for any final typographical errors or minor necessary updates. Please address and answer in full any queries which the copyeditor may have raised on the Author Query sheet accompanying your proofs.

Please make clear any necessary corrections, within **3 working days**, using one of the following methods:

- Use Adobe's Comments and/or Editing Tools to indicate changes directly onto the PDF and return via email. Please request guidelines if required.
- Email the necessary corrections as a list citing the page and line number where a correction needs to be made, how the text currently appears, and what it should be changed to.
- Use the BSI proof marks to indicate changes on a paper printout of the PDF and email, fax or post the pages (contact details below).

Production Editor, mst, 1 Carlton House Terrace, London, SW1Y 5AF, UK, Tel.: 44 (0)20 7451 7359 Fax: 44 (0)20 7451 7307
mst@maneypublishing.com

VIEWING YOUR ARTICLE'S PRODUCTION STATUS AND PLACING ORDERS USING MANEYTRACK

http://maneytrack.maney.co.uk

Approximately three weeks ago, you will have received an email detailing your log-in details for Maney Publishing's web-based production tracking system, ManeyTrack. Via ManeyTrack you can:

- View the production status of your article at any time.
- Place orders for printed colour, offprints, issue copies, or to make your article open access.

Please log in using the web address, above. If you have misplaced your log-in details please check your spam/junk folder. If you are still unable to find them please click on the above url and click on 'Forgot Password' and follow instructions. If you require further technical assistance, please contact the Administrator: ManeyTrackAdmin@maneypublishing.com

ADDITIONAL INFORMATION

This journal is hosted online at www.maneyonline.com/mst

ADVANCE ARTICLES: Once your corrections have been returned a corrected version of your paper will be published online within three weeks and you will receive a notification email. Once your article is published on Advance Articles it will only be available to you if your institution subscribes to the journal or if you have a personal subscription. However, once it has been published in an issue you will receive by email a complimentary PDF eprint of the final version. For further information about Advance Article publication please see www.maneyonline.com/page/authors/afteracceptance

OPEN ACCESS (MORE OpenChoice): Should you wish to make your article freely available online (open access) please log in to ManeyTrack to view prices and to place your order – see details for ManeyTrack above. For more information regarding Maney's open access product, MORE OpenChoice, please see: www.maneyonline.com/openaccess

OFFPRINTS: You will receive a complimentary PDF eprint of your final article. If you wish to purchase traditional hardcopy offprints please log in to ManeyTrack to view prices and to place your order – see details for ManeyTrack above.

ISSUE COPIES: You will have the opportunity to purchase a copy or copies of the issue your article will be published in at the time you receive the final PDF (eprint) of your article. Details stating how to order will be included in the eprint email.

PRINTED COLOUR: All figures supplied as such will be reproduced online in colour free of charge. If you would like colour figures reproduced in the printed version please log in to ManeyTrack to view prices and to place your order – see details for ManeyTrack above.

FEEDBACK

As part of our commitment to improving the experience of authors publishing with Maney, and to maintain the high standards of the journals we publish, we would like to invite authors of recently published papers to take part in our survey.

The survey takes less than five minutes to complete.

Science and healthcare authors please use this link
https://www.surveymonkey.com/s/stm_authorsurvey

***Please note this PDF file may not be offered for commercial sale or for any systematic external distribution by a third party.**

Kind regards,
Production Editor

Cyclic deformation and microstructural behaviour of reduced activation ferritic–martensitic steels

M. N. Batista, I. Alvarez-Armas, M. F. Giordana, S. Hereñú and A. F. Armas

The present paper presents results about cyclic behaviour and the evolution of the dislocation structure of reduced activation ferritic–martensitic steels and commercial martensitic steels AISI 410 and 420. The variation of the free dislocation density within subgrains and subgrain size was mainly analysed during the cyclic softening of EUROFER 97 steel. From the analysis of the flow stress components, the friction and back stresses, and the information of the evolution of the dislocation structure, it could be concluded that the softening of tempered martensitic steels at 20°C is produced by the contribution of the friction stress and aided later by the back stress.

Keywords: RAFM steels, Martensitic steels, LCF, Microstructure, Dislocations

Introduction

Ferritic steels, commercial 9–12%Cr martensitic and 2·25%Cr bainitic steels, were first considered for fusion reactors in the late 1970s because of their excellent thermal properties and radiation resistance.[1] In the mid-80s, a new class of structural materials, namely, the reduced activation ferritic–martensitic (RAFM) steels, was developed.[2] During service, blanket modules of International Thermonuclear Experimental Reactor are subject to alternating thermal and mechanical stresses, as a consequence of the reactor operation. Therefore, fatigue loading behaviour of blanket modules manufactured from reduced activation RAFM steels is a primary concern.

Previous low cycle fatigue (LCF) studies on 9–12Cr steels showed that cyclic softening occurs due to microstructural instability over a wide range of temperatures, from room to high temperature.[3–13] This effect could become a serious engineering problem affecting creep, swelling and segregation phenomena during irradiation. Cyclic softening of 9–12Cr steels is associated with instability of the dislocation structure over the entire range of temperatures and with the coarsening of carbides at high temperatures.

Nowadays, the softening stage in 9–12Cr steels and especially in RAFM steels is clearly associated with the increase in the subgrain size regardless of the temperature.[10] Moreover, the softening has been at least partially explained by lath and subgrain boundary elimination.[14] The softening stage has been also described by an empirical power law equation, which is independent of the applied total strain amplitude and only dependent on temperature.[4] However, a correlation between cyclic behaviour and dislocation structure evolution has hardly been treated.

The aims of the present paper are to correlate the cyclic deformation behaviour with microstructural parameters for RAFM steels and to compare these results to those from commercial martensitic steels.

Experimental

The materials considered in the present study were the RAFM steels EUROFER 97, F82H mod and commercial AISI 410 and 420 steel. Tables 1 and 2 show the chemical composition of these steels in weight per cent and the heat treatments and mode of cooling in each case used before testing respectively.

The microstructure of all steels consists of a tempered martensitic lath structure composed of small subgrains with a substantial dislocation structure. $M_{23}C_6$ carbides were distributed preferentially along laths and prior austenitic grain boundaries. It is interesting to note that the high dislocation density produced during the quenching of the steels remains after tempering.

Low cycle fatigue tests of EUROFER 97 and F82H have been performed under total strain controlled conditions using a triangular wave form. Experiments were performed over total strain ranges of $\Delta\varepsilon_t$=0·6, 0·8, 1·0 and 1·5%, which corresponds to a plastic strain range of approximately to $\Delta\varepsilon_p$=0·1, 0·3, 0·5 and 1·0% at middle life respectively, with a total strain rate $\dot{\varepsilon}=3\times10^{-3}$ s^{-1}. Solid specimens with a cylindrical gauge section 77 mm in length and 8·8 mm in diameter were deformed. The gauge length of the axial extensometer was 21 mm.

In order to study the microstructural parameters in EUROFER 97, cyclic tests were performed under plastic strain control over the strain ranges of $\Delta\varepsilon_p$=0·2, 0·3 and 0·6%. Only a single plastic strain range of $\Delta\varepsilon_p$=0·2% was for AISI 410 and 420 with a total strain rate of $\dot{\varepsilon}=2\times10^{-3}$ s^{-1} up to fracture. Additionally, interrupted

Instituto de Física Rosario, CONICET-UNR, Bv. 27 de Febrero 210 bis, Rosario 2000, Argentina

*Corresponding author, email alvarez@ifir-conicet.gov.ar

Published by Maney on behalf of the Institute
Received 27 November 2013; accepted 23 December 2013
DOI 10.1179/1743284713Y.0000000490

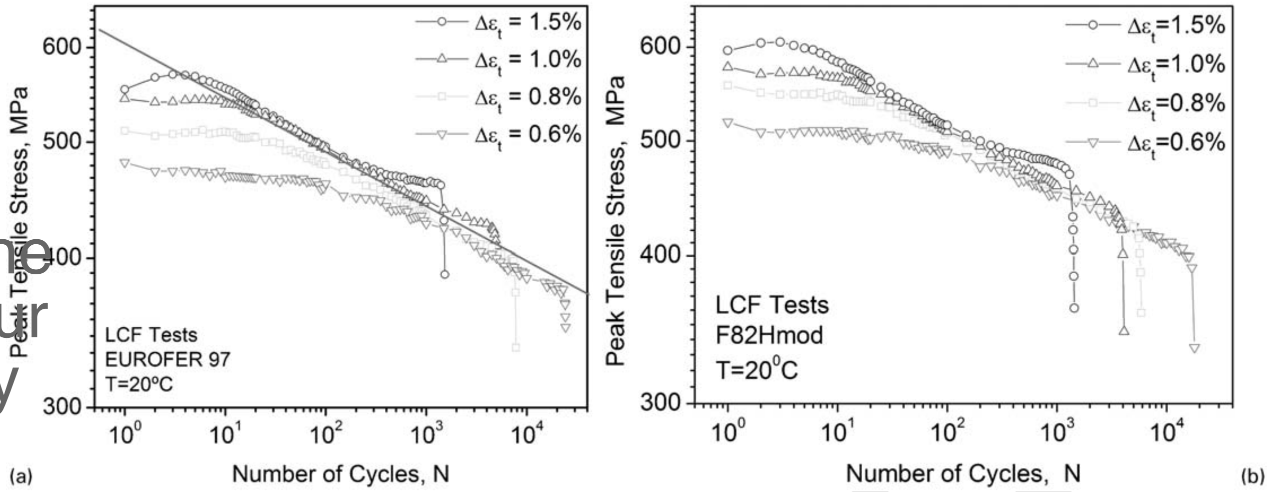

1 Peak tensile stress plotted against number of cycles of *a* EUROFER 97 and *b* F82H mod

tests for a plastic strain range of $\Delta\varepsilon_p = 0{\cdot}2\%$ have been carried out up to 10 and 500 cycles.

EUROFER 97 and AISI 420 specimens cycled under plastic strain control were examined by transmission electron microscopy (TEM) using a 100 kV microscope. Transversal discs were cut from the gauge length of the specimen and then electrolytically thinned for TEM observations.

Results and discussion

Cyclic softening curves were obtained from testing EUROFER 97 and F82H mod specimens at 20°C in the above mentioned total strain range. Figure 1 shows these results plotted in as log–log diagrams. Similar softening tendencies are observed for all the ranges, i.e. a transitional stage corresponding to the first part of the fatigue life followed by a linear second stage that occupies the main part of the life and finally a saturation stage ($\Delta\varepsilon_t = 1{\cdot}5\%$) occurs. Actually, in a number of tests, the final crack nucleates and grows before the saturation stage can occur, which the dislocation structure is already stable. These results correspond to similar results obtained previously by the authors, but not yet totally published.[4,5] These results have shown that, for different temperatures, RAFM steels present the same cyclic behaviour (line traced on Fig. 1*a*). In this respect, Armas *et al.* have demonstrated that the linear or main stage exhibited by these curves is almost independent of the total strain range at each temperature.[5] This linear stage follows a power law equation between the applied stress and the number of cycles

$$\sigma = AN^{-s} \qquad (1)$$

where σ is the peak tensile stress of the hysteresis loop, N is the number of cycles, S is the cyclic softening coefficient and A is a constant that depends on temperature. S is the slope of the linear stage in the log–log diagram. It represents the magnitude of the cyclic softening, and the pre-exponential factor A is the y-intercept in this diagram.

Figure 2 illustrates the behaviour of the cyclic softening coefficient as a function of temperature, S versus T, for several RAFM and commercial steels. It is interesting to note that the coefficients for RAFM steels lie on the same curve, while the commercial steels fit another curve of the same type, but with lower softening coefficient values.

A martensitic lath structure with a high density of entangled dislocations lying within the laths is characteristic of normalised and tempered steels with high martensitic start M_S temperatures. It is known that chemical composition is the main factor affecting the M_S temperature of the steel. Reduced activation ferritic–martensitic steels such as EUROFER 97 and F82H with lower amounts of C, Ni, Mo and Nb are steels with a high M_S temperature and, consequently, with a high dislocation density within their structure. A higher M_S temperature produces a higher dislocation density

Table 1 Chemical compositions in wt-%

Steels	C	N	Si	Mn	Ni	Cr	Mo	W	V	Ta	Nb	Al	Ti	Cu	Fe.
EUROFER 97	0·12	0·018	0·06	0·47	0·022	8·93	0·0015	1·07	0·2	0·14	…	0·008	0·01	0·004	Balance
F82H mod	0·09	0·007	0·11	0·16	0·019	8·16	0·002	2·2	0·15	0·02	0·0001	0·02	0·002	0·006	Balance
AISI 410	0·11	–	0·47	0·7	0·38	13	…	…	…	…	…	…	…	…	Balance
AISI 420	0·27	–	0·36	0·35	0·13	12·3	0·07	…	0·04	…	0·03	…	…	…	Balance

Table 2 Heat treatments of steels: austenitisation/air cooling and tempering/air cooling

RAFM steels	Austenitisation	Tempering	Comm. steel	Austenitisation	Tempering
EUROFER 97	980°C/0·5 h	760°C/1·5 h	AISI 420	1000°C/0·5h	760°C/1·5h
F82H mod	1040°C/ 0·5 h	750°C/ 2 h,	AISI 410	1000°C/0·5h	760°C/1·5h

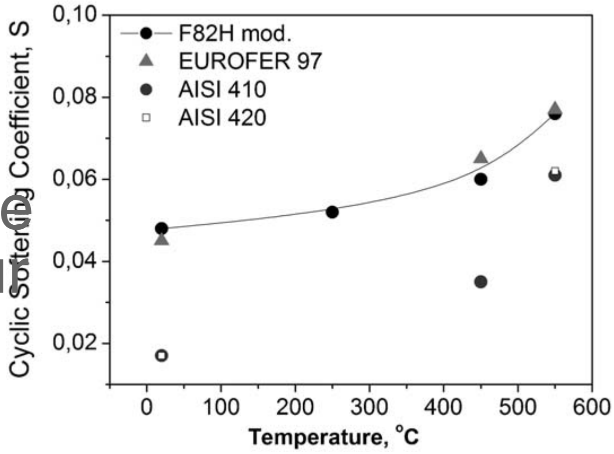

2 Cyclic softening coefficient plotted against temperature for several martensitic steels, RAFM and commercial steels

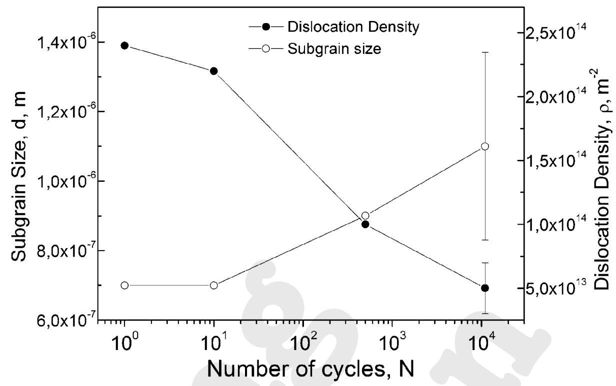

3 Variation of subgrain size and free dislocation density of EUROFER 97 against number of cycles

within the subgrains that compose the lath structure. In low carbon steels, under cyclic conditions, this structure gradually transforms from a narrow lath structure to a subgrain structure of different sizes depending on the deformation strain range and temperature. Table 3 summarises the M_S temperature as well as the pre-exponential factor A and cyclic softening coefficient S for different temperatures. The M_S temperature was calculated on the basis of the equation proposed by Steven–Haynes[15]

$$M_S(^\circ C) = 561 - 474(\%C) - 33(\%Mn) - 17(\%Ni) - 17(\%Cr) - 21(\%Mo) \qquad (2)$$

Table 3 Martensitic start temperature M_S, cyclic softening coefficient S and pre-exponential factor A for selected RAFM as well as commercial steels during total strain control cycling

		20°C	550°C
F82H	M_s	370°C	
	A	635	422
	S	0·048	0·076
EUROFER 97	M_s	365°C	
	A	630	396
	S	0·045	0·077
AISI 410	M_s	258°C	
	A	575	575
	S	0·038	0·038
AISI 420	M_s	203°C	
	A	480	360
	S	0·017	0·062

Observations by TEM and analysis of the microstructure from specimens cycled for a different number of cycles have been carried out according to Table 4 and plotted in Fig. 3 to correlate the cyclic flow stress with the variation of the microstructural parameters such as free dislocation density and subgrain size. This graphic clearly shows the rate at which subgrain size and dislocation density change during cycling.

Following Table 4, the relationship between subgrain size d and free dislocation density ρ have been plotted in a log–log diagram in Fig. 4; a double error bar was added in order to estimate measurement dispersion in these parameters. In this graph, the data corresponding to the specimens cycled at $\Delta\varepsilon_p$=0·2% and T=20°C for three different numbers of cycles in the softening stage act as a basis to compare these results with those obtained at other strain ranges, temperatures and steels. It is worth noting that irrespective of the plastic strain range, the microstructural data of EUROFER 97 fits fairly well the same straight line, with a slope equal to −0·3, in a log–log plot. The data for d and ρ for a higher plastic strain range have been assumed to be close to that for $\Delta\varepsilon_p$=0·2% because of the slight variation of the applied stress at the beginning of the softening stage (N=10 cycles). In the case of high temperature, T=550°C, the softening stage starts from the beginning of the test, i.e. N=2, and continues up to rupture.[5] Thus,

Table 4 Microstructural data (subgrain size d and free dislocation density within subgrains ρ) obtained from LCF tests carried out on specimens cycled over different ranges under plastic strain control $\Delta\varepsilon_p$ for different number of cycles N and at rupture N_f: number of measured subgrains is also given n

		Initial	20°C					550°C
$\Delta\varepsilon_p$	(%)	…	0·2	0·2	0·2	0·3	0·6	0·2
N		0	10	500	N_f=11 000	N_f=7500	N_f=2300	N_f=4000
EUROFER 97	d/m	$0·7\times10^{-7}$	$0·7\times10^{-7}$	$0·9\ 10^{-7}$	$1·1\times10^{-7}$	$1·2\times10^{-7}$	$1·3\times10^{-7}$	$2·1\times10^{-7}$
	n	960	780	693	562	644	418	204
	ρ/m^{-2}	[illegible]	[illegible]	$1·0\times10^{8}$	$0·5\times10^{14}$	$0·5\times10^{14}$	$0·4\times10^{14}$	$0·2\times10^{14}$
	n	21	18	21	28	25	28	26
N		0			N_f=1100			N_f=1050
AISI 420	d/m	$1·0\times$[illegible]	[illegible]	[illegible]	$1·3\times10^{-7}$	…	…	$2·2\times10^{-7}$
	n	2200	…	…	1100	…	…	1050
	ρ/m^{-2}	$2·2\times10^{14}$	…	…	$0·5\times10^{14}$	…	…	$0·1\times10^{14}$
	n	18	…	…	21	…	…	26

d [m]
ρ [m-2]
d [m]
ρ [m-2]

Online colour only

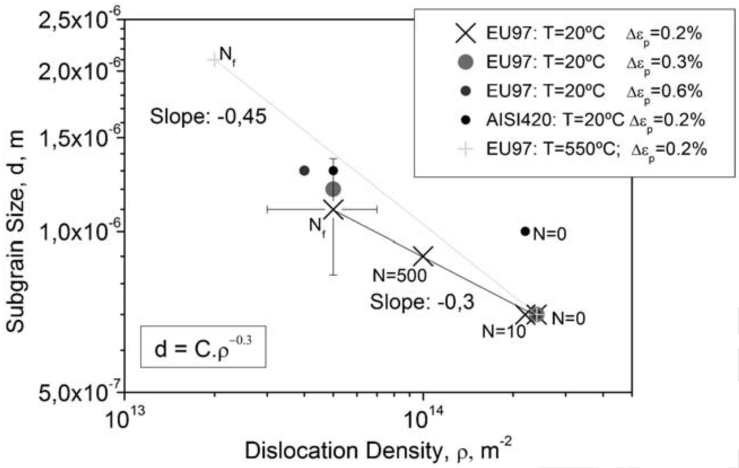

4 Empirical correlation of dislocation subgrain size in cycled EUROFER 97 and AISI 420 steels with average dislocation density

according to the linear law ruling, the applied stress as a function of the numbers of cycles in a log–log plot, it is reasonable to calculate the relationship between d and ρ directly from the data before cycling and at the end of the test. The value of this slope is $-0{\cdot}45$. Note that, for commercial steels, i.e. AISI 420, even though the initial subgrain size is larger than in the case of EUROFER 97, the final values (ρ, σ) agree with those of EUROFER 97 at rupture. In the case of AISI 410, not included in this graph for clarity reasons, the initial size is comparable to that of EUROFER 97.[16] This fact agrees with AISI 410's higher M_S temperature when compared with AISI 420. The same relationship, slope $-0{\cdot}3$, between subgrain size and dislocation density has also been proposed by other authors for copper, aluminum and iron.[17]

According to Table 4, Fig. 5*a* shows the behaviour that follows the evolution of the peak tensile stress with the inverse of the subgrain size during softening. This figure shows that the slope of the line is about 10 times (**b**G), where **b** is the Burgers vector and G is the shear modulus

$$\sigma = 10(\mathbf{b}G)/d \tag{3}$$

This means that, during LCF of RAFM steels, the applied stress and subgrain diameter are inversely related following an expression similar to that calculated by Orowan for the interaction between dislocations and particles. The same relation was previously proposed for the saturation stress subgrain size during fatigue of polycrystalline copper and irons[17] and for the steady state subgrain size during creep for many materials including tempered martensitic steels.[11]

Figure 5 shows that a log–log plot of the peak tensile stress versus the square root of the free dislocation density follows a linear whose slope is close to 1/3 for room temperature. Therefore, the power law equation that fits this curve is

$$\sigma = C\rho^{1/6} \tag{4}$$

where C is the pre-exponential factor.

The power equation that governs the applied stress against the square root of the dislocation density equation (4) can be understood considering the behaviour of the stress components during fatigue.[18] The flow stress obtained from the hysteresis loops is the result of two kinds of resistance to plastic deformation: a short distance interaction stress named the 'friction

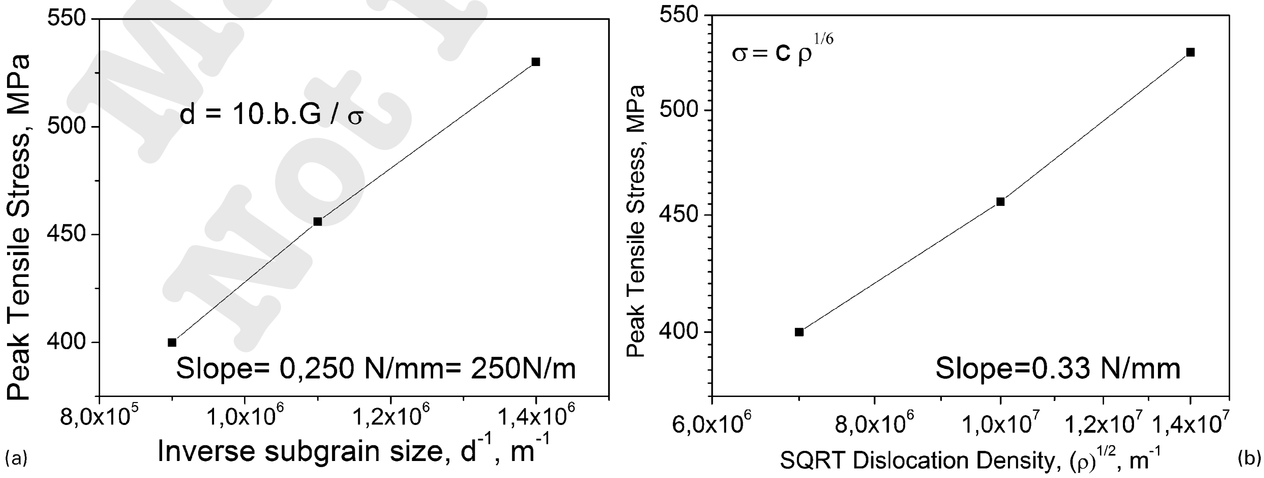

a peak tensile stress against inverse of subgrain size; *b* peak tensile stress against square root free dislocation density

5 EUROFER 97 cycled at $\Delta\varepsilon_p$=0·2% at T=20°C

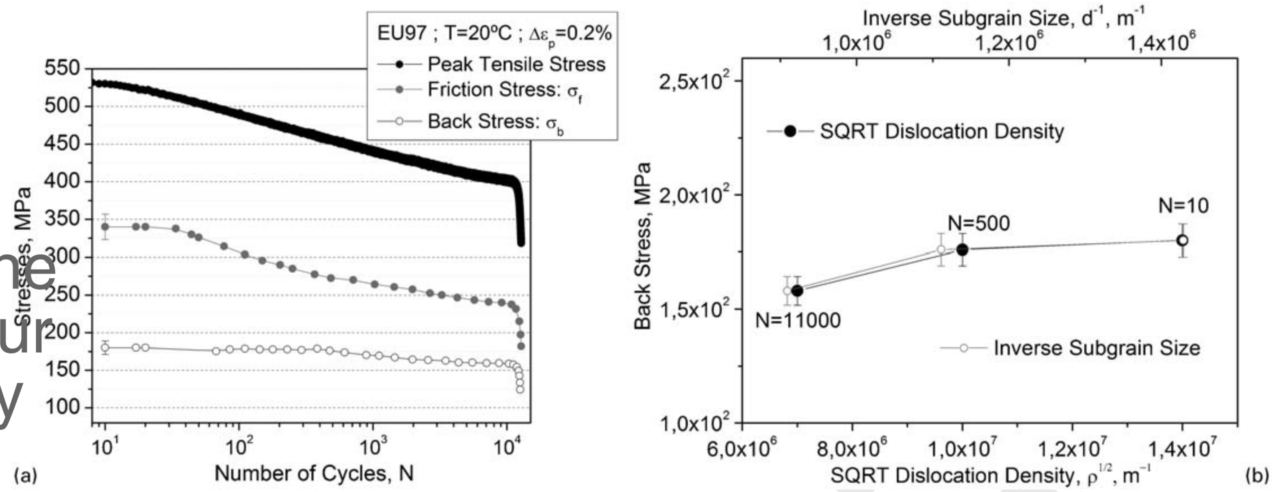

Online colour only

6 ***a*** **cyclic stress components behaviour of EUROFER 97 at 20°C and** ***b*** **back stress against inverse subgrain size and square root of free dislocation density**

stress' σ_f and a long distance interaction stress called the 'back stress' σ_b.

The behaviour of the cyclic stress components of EUROFER 97 at 20°C are represented in Fig. 6*a*. In this graph, there is clear evidence of a pronounced decrease in the σ_f when compared to the σ_b over the fatigue life, which only represents a slight decrease from 500 cycles up to rupture. This fact means that the interaction of dislocation with short range obstacles is an important softening mechanism during the entire room temperature fatigue. However, the interaction with long range obstacles is significant only after ~500 cycles. Short range obstacles are associated with foreign atoms and other dislocations, while long range obstacles are related to borders (grain, subgrain/lath walls, etc).

In Fig. 6*b*, the behaviour of the stress component responsible for long range interactions σ_b is plotted against both the square root of free dislocation density and the subgrain size. These curves exhibit a weak dependence of σ_b on both the subgrain size and the dislocation density in approximately the first 500 cycles. Comparing this behaviour of the back stress with that of the friction stress as a function of the SQRT dislocation density,[9] one can conclude that the softening stage can be subdivided in two processes, one mainly due to the annihilation of free dislocations during the fatigue life and the other due to the annihilation of subgrain boundaries after certain number of cycles. It is worth mentioning that the later process is more remarkable at higher temperatures. This characteristic number of cycles in which a second mechanism is activated, can be estimated from the σ_b curve (Fig. 6*a*); it shows a moderately decreasing values of this stress from 500 cycles up to rupture (of ~12%). Comparing this behaviour with the variation of the subgrain size, and taking into account the great dispersion of these values (Fig. 3), one could conclude that the influence of the subgrain size increase is relevant in the same order as σ_b is.

Figure 7*a* and *b* shows the characteristic lath structures of the material after tempering in which the dislocation subgrain has a high density of free dislocations in its interior. After 10 cycles, the number of

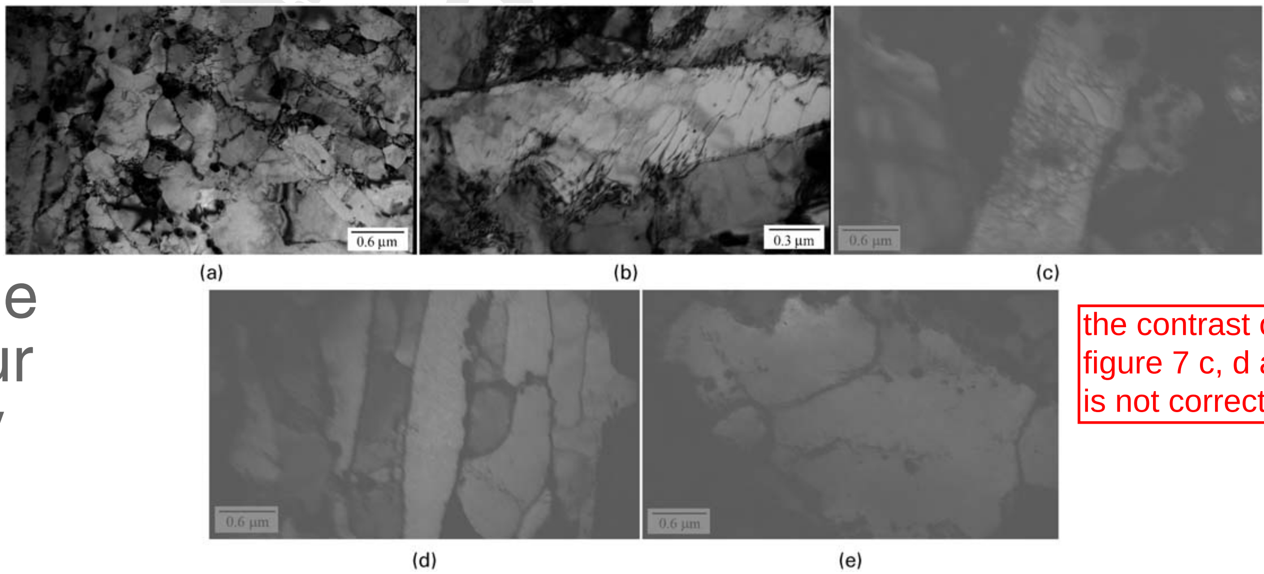

Online colour only

the contrast of figure 7 c, d and e is not correct

7 EUROFER 97: ***a*** **characteristic lath structures after tempering and** ***b*** **lath unit showing high density of free dislocations in its interior after** ***c*** **10 cycles,** ***d*** **500 cycles and** ***e*** **rupture**

moving dislocations is still high (Fig. 7*c*), in contrast to Fig. 7*d* in which the subgrain interior is cleaner and the walls start to be more refined. Therefore, cycling at RT induces two visible microstructural evolutions; first and the most important, the free dislocation density decreases during cycling (compare Fig. 7*b*–*d*). Second, dislocation walls are well defined and some disappear during cycling, which explains their growth. Figure 7*e* gives clear evidence of coarsening of the subgrain structure, first refining and then annihilating dislocation walls as is predicted by the applied stress components.

Briefly correlating cyclic softening and microstructural behaviour, it was found that the characteristic cyclic softening behaviour observed for RAFM steels can be described by a softening parameter S that is only dependent on temperature.

At 20°C, a characteristic subgrain size seems to be attained at the end of the fatigue life for specimens cycled at different applied strain amplitudes.

In fact, tempering is a process in which the microstructure approaches equilibrium under the influence of thermal activation. It follows that the tendency to temper depends on how far the starting microstructure deviates from equilibrium. The excess of an element such as carbon, which is forced into solution in martensite is the major contributor to the stored energy of martensite. Previous investigations[19] have reported the microstructural stability of normalised and tempered 9–12%Cr modified martensitic steels during subsequent annealing times up to 1100 h at 550°C. However, this apparent microstructural stability could be destabilised under cyclic strain conditions, as many authors have discussed in the literature. The apparently stable tempered lath martensite structure is strongly unstable under cyclic conditions, being gradually replaced by the development of a subgrain structure. The evolution of the typical tempered martensite lath structure of low carbon alloy steels to a subgrain structure was reported to be already established after only a few cycles.[10]

Therefore, it is evident that the tempering process lowers the stored energy in the martensitic structure to a level that cannot decrease further even after longer heat treatment times.[19] However, the result of cycling makes the subgrain size increase and the dislocation density decrease, and these tendencies are still more pronounced when cycling is carried out at higher temperature. Hence, in this process, temperature assists cycling to more effectively reduce the internal energy stored during the martensite structure formation. This synergism could explain the fact that regardless of the applied strain range, at a given temperature, the subgrain size tends to attain a stable value.

Conclusions

The present investigation correlates cyclic softening with the microstructural evolution of RAFM and commercial steels at 20°C.

1. The commercial steels exhibit lower softening parameters S compared with RAFM steels.
2. The annihilation of free dislocations mainly contributes to the softening behaviour as reflected by the friction stress. In addition, the annihilation of subgrain boundaries can be considered as a second mechanism activated later in this process.
3. Final subgrain size is dependent on the available stored energy that still remains after the tempering process and which decreases to a lower level during cycling.

Acknowledgement

This work was supported by the Agencia Nacional para la Promoción de la Ciencia y la Técnica (ANPCyT) and Consejo Nacional de Investigaciones Científicas y Técnicas (CONICET) of Argentina.

References

1. R. L. Klueh and A. T. Nelson: 'Ferritic/martensitic steels for next-generation reactors', *J. Nucl. Mater.*, 2007, **371**, 37–52.
2. A. F. Rowcliffe, E. E. Bloom, D. G. Dorand, D. L. Smith and T. C. Reuther: 'Low activation materials for fusion', Proc. 20th Int. Conf. on 'Plasma physics and controlled nuclear fusion research, Nice, France, IAEA, October 1988. 2
3. A. F. Armas, M. Avalos, I. Alvarez-Armas, C. Petersen and R. Schmit: 'Dynamic strain aging evidences during LCF deformation in ferritic–martensitic steels', *J. Nucl. Mater.*, 1998, **258–263**, 1204–1208.
4. A. F. Armas, C. Petersen, R. Schmitt, M. Avalos and I. Alvarez: 'Mechanical and microstructural behavior of isothermally and thermally fatigued ferritic/martensitic steels', *J. Nucl. Mater.*, 2002, **307–311**, 509–513.
5. A. F. Armas, C. Petersen, R. Schmitt, M. Avalos and I. Alvarez: 'Cyclic instability of martensite laths in reduced activation ferritic/martensitic steels', *J. Nucl. Mater.*, 2004, **329–333**, 252–256.
6. M. F. Giordana, I. Alvarez-Armas, M. Sauzay and A. F. Armas: 'Mechanical behavior and microstructure evolution of EUROFER 97 during low-cycle fatigue at 20 and 550°C', *Key Eng. Mater.*, 2011, **465**, 358–361.
7. M. F. Giordana, P.-F. Giroux, I. Alvarez-Armas, M. Sauzay and A. F. Armas: 'Micromechanical modeling of the cyclic softening of EUROFER 97 steel', *Procedia Eng.*, 2011, **10**, 1268–1273.
8. M. F. Giordana, P.-F. Giroux, I. Alvarez-Armas, M. Sauzay, A. F. Armas and T. Kruml: 'Microstructure evolution during cyclic tests on EUROFER 97 at 20°C. TEM observation and modeling', *Mater. Sci. Eng. A*, 2012, **A550**, 103–111.
9. M. F. Giordana, I. Alvarez-Armas and A. F. Armas: 'Microstructural characterization of EUROFER 97 during low cycle fatigue', *J. Nucl. Mater.*, 2012, **424**, 247–51.
10. P. Marmy and T. Kruml: 'Low cycle fatigue of EUROFER 97', *J. Nucl. Mater.*, 2008, **377**, 52–58.
11. J. S. Dubeya, H. Chilukuru, J. K. Chakravartty, M. Schwienheer, A. Scholz and W. Blum: 'Effects of cyclic deformation on subgrain evolution and creep in 9–12%Cr-steels', *Mater. Sci. Eng. A*, 2005, **A406**, 152–159.
12. I. Kubena, B. Fournier and T. Kruml: 'Effect of microstructure on LCF properties of ODS steels', *J. Nucl. Mater.*, 2012, **424**, 101–108.
13. A. A. Saad, W. Sun, T. H. Hyde and D. W. J. Tanner: 'Cyclic softening behavior of a P91 steel under LCF high temperature', *Procedia Eng.*, 2011, **10**, 1103–1108.
14. M. Sauzay, H. Brillet, I. Monnet, M. Mottot, F. Barcelo, B. Fournier and A. Pineau: *Mater. Sci. Eng. A*, 2005, **A400–A401**, 241–244.
15. W. Stevens and A. G. Haynes: 'The temperature of forming martensite and bainite in low-alloy steels', *ISIJ*, 1956, **183**, 349–359.
16. M. F. Giordana: PhD thesis, University of Rosario, Rosario, Argentina, 2012. 3
17. J. C. Grosskreutz and H. Mughrabi: 'Description of the work-hardened structure at low temperature in cyclic deformation', in 'Constitutive equations in plasticity', (ed. A. S. Argon); 1975, Cambridge, MA, MIT Press. 4
18. D. Kuhlmann-Wilsdorf and C. Laird: 'Dislocation behavior in fatigue: friction stress', *Mater. Sci. Eng.*, 1979, **37**, 111–120.
19. W. Jones, C. R. Hills and D. H. Polonis: 'Microstructural evolution of modified 9Cr–1Mo steel', *Metall. Trans. A*, 1991, **22A**, 1049–1058.

Authors Queries

Journal: **Materials Science and Technology**
Paper: **11340**
Title: **Cyclic deformation and microstructural behaviour of reduced activation ferritic–martensitic steels**

Dear Author
During the preparation of your manuscript for publication, the questions listed below have arisen. Please attend to these matters and return this form with your proof. Many thanks for your assistance

Query Reference	Query	Remarks
1	Please confirm the running head is correct.	correct
2	Please confirm additional information for Ref. 2 and supply page/paper no.	Report Number: IAEA-CN-50/G-III-2; p.429
3	Please supply title of thesis for Ref. 16.	ABLANDAMIETO CÍCLICO DE ACEROS AVAZADOS: BASE EXPERIMETAL Y MODELIZACIÓN
4	Please supply page for Ref. 17.	p.p. 251-326